esa

ECOSPHERE

Terrestrial mammal three-dimensional photogrammetry: multispecies mass estimation

M. Postma,[1] A. S. W. Tordiffe,[2,3] M. S. Hofmeyr,[4] R. R. Reisinger,[1] L. C. Bester,[1] P. E. Buss,[4] and P. J. N. de Bruyn[1,†]

[1]*Mammal Research Institute, Department of Zoology and Entomology, University of Pretoria, Private Bag X20, Hatfield 0028 South Africa*
[2]*Department of Research and Scientific Services, National Zoological Gardens of South Africa, Box 754, Pretoria 0001 South Africa*
[3]*Department of Companion Animal Clinical Studies, Faculty of Veterinary Science, University of Pretoria, Onderstepoort 0110 South Africa*
[4]*Veterinary Wildlife Services, South African National Parks, Kruger National Park, Skukuza 1350 South Africa*

Citation: Postma, M., A. S. W. Tordiffe, M. S. Hofmeyr, R. R. Reisinger, L. C. Bester, P. E. Buss, and P. J. N. de Bruyn. 2015. Terrestrial mammal three-dimensional photogrammetry: multispecies mass estimation. Ecosphere 6(12):293. http://dx.doi.org/10.1890/ES15-00368.1

Abstract. Assessing body mass in mammals is of importance as it influences virtually all aspects of mammal physiology, behavior and ecological parameters. However, the assessment of body mass of large mammals is potentially dangerous and logistically challenging. Photogrammetry (measurements through the use of photographs) is a well-established science. In zoology it has been used with varying success to estimate the size and mass of some marine and terrestrial mammal species. However, photogrammetric body mass estimation of terrestrial mammals has received comparatively little attention. This is largely due to species' variable morphological attributes which complicates measurement especially if, for 3D orientation, photogrammetric models are dependent on identifiable features on the animals themselves. Ninety-two individuals belonging to 16 terrestrial mammalian species were weighed and photographed for body mass estimation using a volumetric photogrammetry method, purposely applied with commercially available software. This method is not dependent on identifiable body features for 3D orientation. Measured body mass ranged from 25 kg to 4060 kg. Photogrammetric mass estimates versus physically weighed mass was plotted and the goodness of fit assessed for each species. Body size, shape and physiological attributes influence the accuracy of body mass estimation between species (although consistent within species), largely attributed to morphological features (e.g., hair length and posture). This photogrammetric method accurately estimated the body mass of several terrestrial mammal species. It represents innovative use of photographs to create calibrated three-dimensional imagery for accurate quantification of mammalian metrics, specifically body volume and mass. Advances of a method that is not subject to species, sex or age is advantageous and suitable for wide application in our effort to model population demography.

Key words: ecological method; field technique; large mammals; mass estimation; photogrammetry; remote measurement; terrestrial mammals.

Received 12 June 2015; accepted 23 June 2015; **published** 22 December 2015. Corresponding Editor: D. P. C. Peters.

† **E-mail:** pjndebruyn@zoology.up.ac.za

Introduction

Broadly applicable indirect monitoring methods are favorable in assessing ecological parameters in many zoological studies (e.g., Berger 2012, McCallum 2013, Postma et al. 2013*a*, Purves et al. 2013). Such methods aim to: minimize contact and manipulation and thus disturbance of wild animals; attempt to reduce financial and manpower needs, while maintaining accuracy and efficiency; and should preferably allow the collection of large samples of data. Monitoring wild populations of large mammals poses unique challenges to researchers; particularly difficult for data collection being the physical attributes of body mass and size. Knowledge of body mass and size is central to the majority of anatomical, physiological or behavioral life history studies (Alexander and Goldspink 1977). Change in body mass specifically has regularly been used to quantify individual productivity in both marine (e.g., Postma et al. 2013*b*) and terrestrial mammals (e.g., Clutton-Brock et al. 1989, Festa-Bianchet et al. 1998). In general, heavier individuals survive better (Gaillard et al. 1997, 2000, McMahon et al. 2000) and produce larger offspring who gain similar benefits (Postma et al. 2013*b*, Zedrosser et al. 2013). Body mass also occupies a central role in thermal regulation, which is coupled to environmental seasonality in that it selects for larger body size, due to increased fasting endurance (Lindstedt and Boyce 1985). Environmental seasonality seems set to exacerbate due to global climate change (Williams and Martinez 2000), making it an imperative, amongst other factors, to monitor body mass changes effectively (Purves et al. 2013). This rearrangement of ecosystems due to climate change will inevitably have an influence on productivity and survival of wild populations. Changes in the productivity of ecosystems will influence body mass and size of primary consumers such as mammalian herbivores. However, monitoring mass change in wild terrestrial large mammals remains challenging; hampered by inaccessibility, size and behavior of many species. Traditionally, body mass is assessed directly after physical or chemical immobilization of animals, but this procedure is intrusive, costly and labor intensive. Consequently, when even possible, such efforts usually result in limited sample sizes. Researchers and practitioners have looked for alternatives to acquiring these vital data. Advances in modern photography enable the photogrammetric measurement of morphological features (e.g., horns and skeletal dimensions), and mass estimation (Haley et al. 1991, Bell et al. 1997, Keith et al. 2001, Lambertsen et al. 2005, Ireland et al. 2006, Schrader et al. 2006, Waite et al. 2007, Bergeron 2007, Rothman et al. 2008, de Bruyn et al. 2009, Postma et al. 2013*a*, *b*). Despite the solid methodological foundation prepared by several of these studies, various limitations to multispecies use of photogrammetry persist in zoology. Recent technological advances can possibly aid in building upon components of these previous methods to alleviate some lingering limitations.

Mammals are a varied ecological group and consequently present an array of physical attributes (morphology) that has direct bearing on the applicability of different physical measuring techniques. This challenge therefore allows mammals, or even subgroups hereof, to be used as a model group to test the applicability of multispecies measuring techniques. Even differences in morphological attributes of a set of large (>10 kg adult body mass) mammal species result in difficulty in formulating a single applicable photogrammetric technique for measurement of all. Such biological diversity underlies the variety of species-specific photogrammetric methods generated for zoological use. The challenge is to progress towards a non-specific technique to facilitate comparative studies. To be of value to conservation, photogrammetry should be practical in a wide range of scenarios and provide robust data that can address a range of important questions (Berger 2012). In short, the method should be applicable to a variety of species.

While several photogrammetric methods use linear measurements (e.g., from paired laser photography; Bergeron et al. 2007) to estimate size of animals with great success and applicability, these remain limited in their linear ability to accurately predict volume or mass without additional data for species-specific morphological regression. Two volumetric estimation three-dimensional (3D) photogrammetry techniques have illustrated particular potential for multispecies applications able to deliver a range of useful linear and non-linear metrics including volume

and mass (Waite et al. 2007, de Bruyn et al. 2009). Both techniques were derived by using pinnipeds as primary target species, utilized different versions of the same 3D modeling software program (Photomodeler Pro) and based volumetric estimations on 3D models derived from the orientation of multiple photographs around the study subjects. Although based on generally similar principles, a small but fundamental difference between these approaches exists. Waite et al. (2007) created 3D models based on the cross-referencing accuracy of orientation landmarks on the study subject (animal) itself, necessitating the use of multiple cameras with simultaneous shutter release stationed around the animal, to effectively 'freeze' the animal in time (i.e., no movement tolerance of the study subject). De Bruyn et al. (2009) were unable to incorporate multiple photographers in their field scenario. This limitation prompted the cross-referencing of stationary landmarks around their study subject to create a highly accurate 3D 'space' unrelated to the study subject, and then modeling the study subject into this 3D space with the use of silhouette tracing. This shift from creating a model based on accurately defined features of the study subject itself to the substrate surrounding the animal was a key methodological advance enabling the method to evolve from a captive controlled environmental application (Waite et al. 2007) to field application by a single camera operator on remote locations (de Bruyn et al. 2009, Postma et al. 2013*a*, *b*). Perhaps most significantly however, the identity and landmark features of the object to be measured are consequently irrelevant as long as an accurate 3D replica (volume) of the real subject was constructed within a calibrated framework (de Bruyn et al. 2009). This advance allows for slight movement of the subject and reduces the number of cameras needed and does not necessarily require modification of the habitat that the study object is located in. However, a lingering limitation is that despite increased tolerance for movement of the study subject (animal) between photographs when using the de Bruyn et al. (2009) method, excessive movement is not permitted. A wild non-immobilized animal, not moving excessively while a photographer moves around it to take photographs, is uncommon. However, southern elephant seals (*Mirounga leonina* (Linnaeus, 1758)) are one such species that are naturally immobile at times, permitting the use and accuracy of the de Bruyn et al. (2009) method. Nonetheless, as illustrated by Waite et al. (2007), the use of multiple cameras stationed around a mobile object can overcome this limitation, and assessments for such multiple camera setups in the field are underway (P. J. N. de Bruyn et al., *unpublished manuscript*). Importantly despite its proposed broad applicability, no quantitative assessment of the accuracy of these two methods for use on a range of mammalian species exists, other than for the two model seal species used to develop the respective methods (Waite et al. 2007, de Bruyn et al. 2009). Clearly, before further research and investment in dealing with the problem of study subject movement (e.g., by multiple-camera setups in the field), the applicability and accuracy of 3D model derived volumetric and mass estimates need to be tested on a larger variety of potential target species.

The aim of this study was therefore to investigate the applicability of the method developed by de Bruyn et al. (2009), and variations thereof, to assess accuracy in photogrammetric estimation of mass for a range of terrestrial mammals. De Bruyn et al. (2009) proposed application of their volumetric method for mass estimation of other large mammal species, given the irrelevance of the identity of the actual study subject for creating an accurate 3D space for measurement. Incorporation of the narrow total body density range of mammals in general (as a consequence of all mammalian tissue cells being made up predominantly of water) as an underlying constant (Durnin and Womersley 1974, Wang et al. 1999), should conceivably allow for mammalian volume estimates to be translated to mass estimates if required.

Furthermore, accuracy is assessed here by simulating a multitude of field scenarios imitating variability of natural settings. By virtue of the fact that accuracy of the photogrammetric method could only be verified by comparison to actual physical measures, all species tested here were immobilized. Although this is directly applicable for when large mammals are immobilized in the field, we furthermore discuss how the results here are fundamental to progress towards a

Table 1. List of abbreviations.

Abbreviation	Description
GPBM	Group predicted body mass
GPE	Group specific predictive equation
MBM	Measured body mass
ME	Mass estimate
PBM	Predicted body mass
PG	Photogrammetry
RMS	Root mean squared
SPBM	Species predicted body mass
SPE	Species specific predictive equation

unified methodological approach for simple photogrammetric size and mass estimation of different large mammals in their natural environments in general, without physical manipulation.

Materials and Methods

Field procedures

Fieldwork was performed at the National Zoological Gardens (NZG) of South Africa and in the Kruger National Park (KNP), South Africa. Photogrammetry (PG; see photogrammetry procedures in Fig. 1 for details; Table 1); the science of making measurements from photographs (Baker 1960), was performed on 92 individuals from 16 mammalian species in captive and field scenarios. Species included: African elephant *Loxodonta africana* (Blumenbach 1797), Arabian oryx *Oryx leucoryx* (Pallas 1777), Bengal tiger *Panthera tigris* (Pocock 1929), bongo *Tragelaphus eurycerus* (Ogilby 1837), cheetah *Acinonyx jubatus* (Schreber 1775), chimpanzee *Pan troglodytes* (Blumenbach 1775), lion *Panthera leo* (Linnaeus 1758), nyala *Tragelapus angasii* (Gray 1849), pygmy hippopotamus *Choeropsis liberiensis* (Morton 1849), red river hog *Potamochoerus porcus* (Linnaeus 1758), sable antelope *Hippotragus niger* (Harris 1838), spotted hyena *Crocuta crocuta* (Erxleben 1777), springbok *Antidorcas marsupialis* (Zimmermann 1780), western lowland gorilla *Gorilla gorilla* (Savage 1847), white rhinoceros *Ceratotherium simum* (Burchell 1817) and zebra *Equus quagga* (Boddaert 1785). Animals were immobilized by the local veterinarian for purposes unrelated to the photogrammetry procedures, varying from surgical to pharmacological studies. Photogrammetry was performed opportunistically after the intended veterinary procedures. In captive zoo scenarios, animals were weighed with a calibrated platform scale (AE 202 Indicator; Adams Equipment, UK). In field scenarios, animals were suspended using broad strapping suspension attached to the feet and weighed with a Loadcell, ULP20t (accuracy 0.1%; and Nagata HC-33; accuracy to closest 1 kg). Animal mass was corrected in all cases for additional strapping and stretchers.

Photogrammetry camera calibration

Prior to use for photogrammetry, each single-lens reflex (SLR) camera (Canon 350D, 400D and 450D) and lens combination is calibrated using a calibration grid with coded targets at a set focal length as described in the calibration manual in the Photomodeler Scanner (EOS Systems, Vancouver, British Columbia, Canada) software package (Postma et al. 2013*a*). Crucially, the calibration procedure is performed at a set focal length (in our case 18 mm) to ensure repeatability in field scenarios (Postma et al. 2013*a*). A structured set of photographs with repeatable settings and parameters are captured, accounting for yaw (e.g., 90 degree rolls) to establish the relationship between the camera body and lens. This is done to ensure the entire field of view is calibrated and to compensate for orthogonal distortion and conversion (Postma et al. 2013*a*). For optimal accuracy, auto-rotation, image stabilizer, and red-eye settings of the camera were switched off for both calibration and field use to reduce unnecessary algorithm calculations (''noise'') during processing (Postma et al. 2013*a*). In an independent comparison of calibration software packages, Photomodeler Scanner calibration procedure was shown to be repeatable and accurate for close range photogrammetry (Remondino and Fraser 2006). During fieldwork, care was taken to ensure photos were taken at calibrated camera settings. Recalibration is only required if the camera or lens is bumped, badly damaged or rebuilt.

Photogrammetry procedure

All subjects could be moved to an even substrate, which made analysis constant (see de Bruyn et al. 2009). All animals were in their natural resting position, ruminants on their sternum, primates on their backs, and carnivores and non-ruminants in lateral recumbence. Following weighing, each animal was photographed

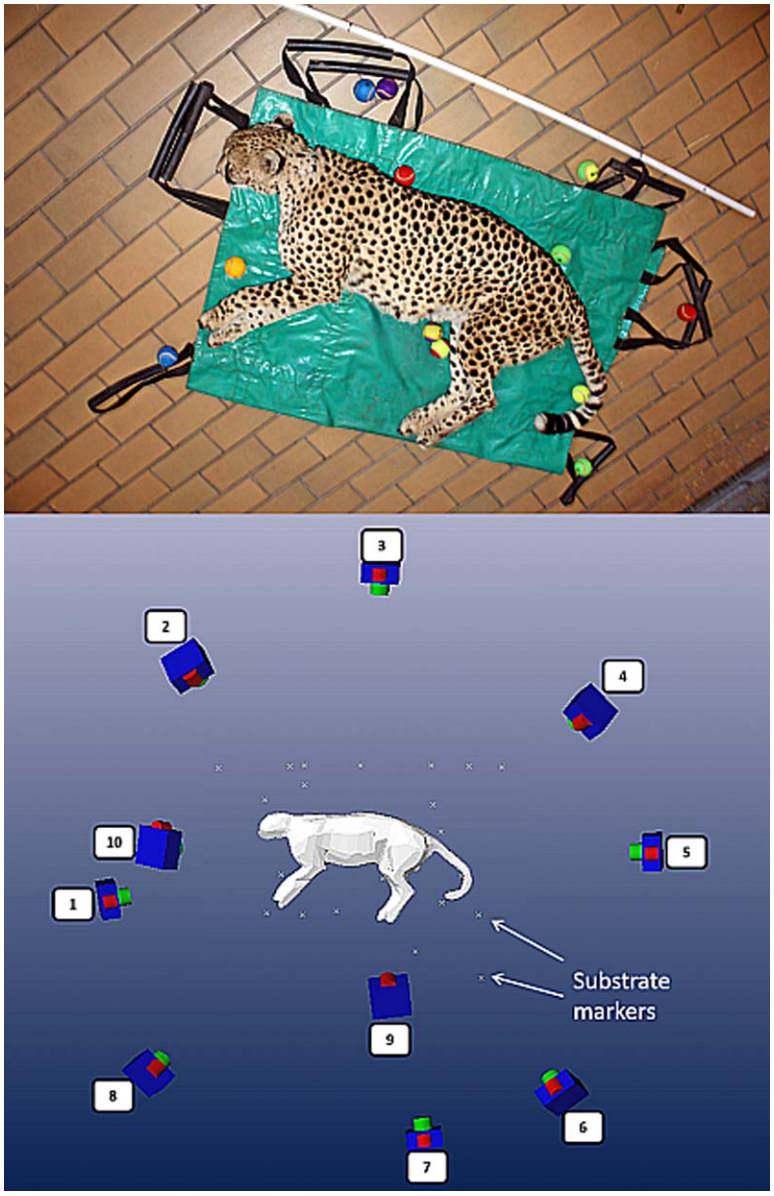

Fig. 1. (Top panel) Photogrammetry set-up example performed on a cheetah. Scale was added by placement of a known length object (2 m long PVC pipe) near the subject so as to be visible in most photographs, and tennis balls were added as substrate markers to facilitate analysis. (Bottom panel) Photomodeler Scanner example three-dimensional model of a cheetah used to estimate body mass. Substrate markers, camera numbers and positioning are indicated.

by a single photographer circling the animal taking 13 photographs from roughly standardized angles relative to the animal (Fig. 1) to form one photogrammetry project. As in de Bruyn et al. (2009), the exact distance of camera stations to the animal or other features in the frame (such as scale measure or substrate markers) need not be measured physically as long as cameras are calibrated. Artificial substrate markers (tennis balls and color coded PVC pipe) were randomly

distributed around the subject to minimize analysis time by simplifying the identification of markers for cross-referencing (see photogrammetric estimation of volume section). Natural markers such as stones and branches can also be used as substrate markers (see de Bruyn et al. 2009). Color coded PVC pipes (2 m) were marked in increments of 50 cm to serve as calibrated scale measure. Importantly, the whole animal and all the substrate markers were included in each photograph where camera angles allowed (see de Bruyn et al. 2009 for allowable alterations). Care was taken during the photogrammetric procedure to ensure no markers were disturbed between photographs taken by the single photographer moving around the subject.

In an independent, stringent evaluation of this software, Deng and Faig (2001) confirmed the high level of accuracy in the creation of the relevant 3D space, justifying its use especially for digital close-range (i.e., $\leq$30 m; i.e., not remote sensing) photogrammetry.

Photogrammetric estimation of volume

Three-dimensional models (based on each of the PG projects) were built using the de Bruyn et al. (2009) method for estimation of body volume and mass. Volumetric estimation procedures were executed using the commercially available 3D modeling package Photomodeler Scanner. From the digital photographs, a 3D spatial model was created using fixed points on the substrate around the animal. These were manually cross-referenced between photographs to create a 3D map of the surrounding substrate. Photographs were sequentially added and manually cross-referenced (starting with three photographs) to ensure maximum orientation precision. The success of a project was evaluated by referring to the software's calculated overall root-mean-squared (RMS) precisions value (pixels) after the addition of each photograph. This marking residual indicates a residual error for each marked point on the photograph (difference between where one places the mark, as facilitated by substrate markers, and where the program expects the mark to be based on the camera calibration information). The mean of marking residuals (hereafters RMS) is considered the best indicator for project quality (Deng and Faig. 2001, de Bruyn et al. 2009; Photomodeler Scanner help files). Once three photographs are orientated with an acceptable RMS ($<$5.0) and anticipated (by the software) processing quality based on various parameters (including number and spacing of substrate markers) is high (between 3 and 5) the project is processed (de Bruyn et al. 2009), after which the procedure is repeated until 13 photographs are included to complete a project. Mapping of the landmarks surrounding the subject contributes to the methods' robustness, as substrate markers remain unmoved between photographs, whereas living (even immobilized) animals are not absolutely still between photographs (breathing, sneezing, etc.). Once all photographs in a project are orientated, the silhouette (outline) of the animal was sequentially traced for each photograph and cross-referenced between photographs to shape the model of the subject (Fig. 1). A series of volumetric measurements were taken after the addition of each new silhouette within a project, to assess when an asymptote is reached. Scale was added by placement of a known length object (2 m long PVC pipe) near the subject so as to be visible in most photographs (see de Bruyn et al. 2009; Fig. 1).

Mass estimation: digestive groups vs. species

The optimum number of photographs to be included in a photogrammetry project was determined for each species by adding photographs to the project until the estimated volume remained constant (Fig. 2). Volume estimates of each individual animal obtained from Photomodeler Scanner was multiplied by a coefficient (1010 kg/m^3); the mean total body density of healthy mammals regardless of total body fat content (Durnin and Womersley 1974, Wang et al. 1999, de Bruyn et al. 2009), to obtain body mass:

$$\mathrm{ME} = \mathrm{Volume}^{\mathrm{Photogrammetric}} \times 1010\ \mathrm{kg/m^3}. \quad (1)$$

The deviation in mass estimate (ME) from photogrammetry volume (kg; % overestimate/percentage error) was calculated for each individual. Consistency of overestimation (percentage overestimate) between individuals within a digestive group was used to assess accuracy of projects. Distinction was made between; foregut-and-hindgut fermenters, carnivores, primates

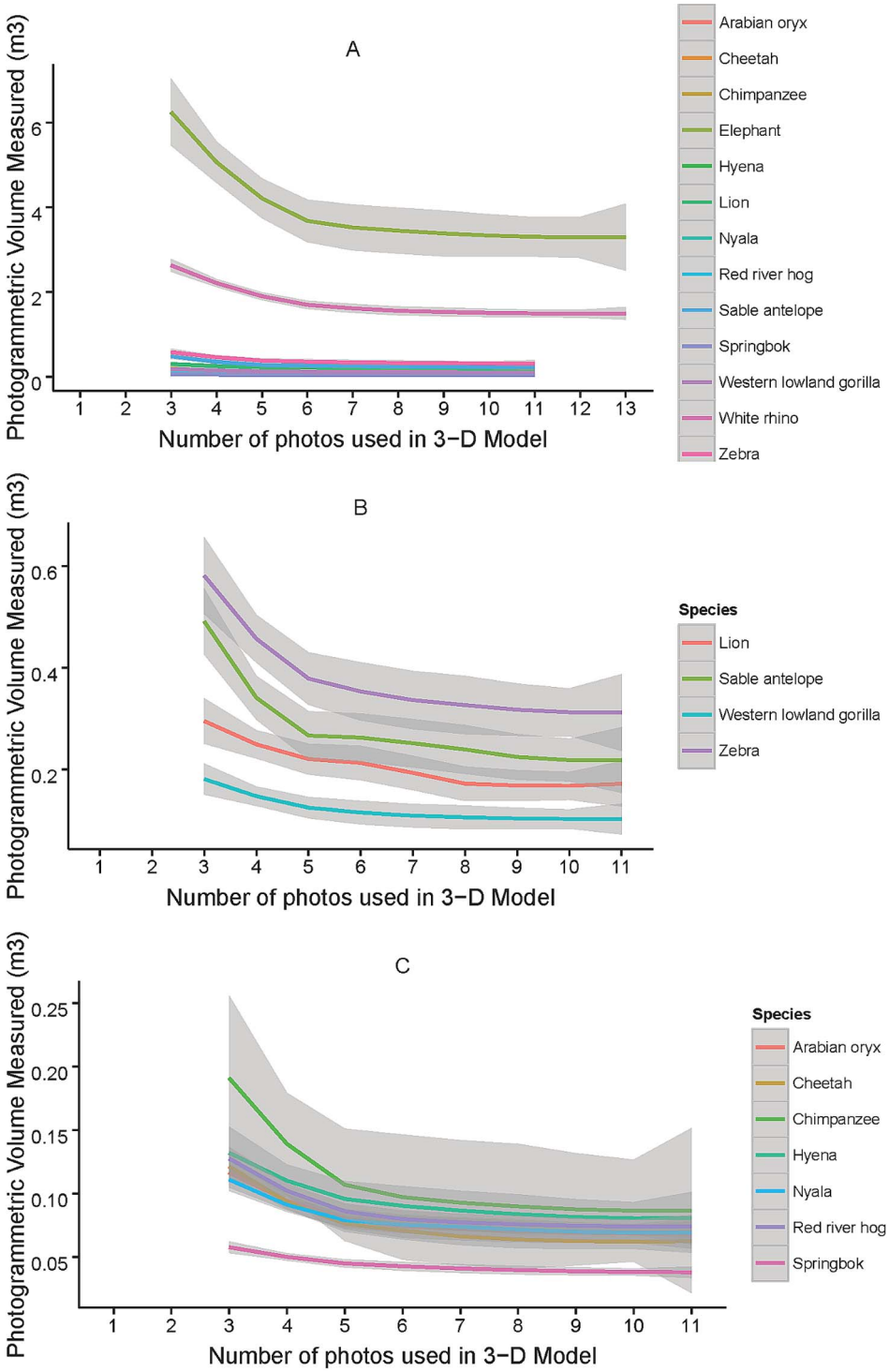

Fig. 2. Species specific volume (m^3) decrease related to number of photographs in a photogrammetry project: mean volume per species is indicated by the colored lines and the shaded area shows the standard deviation range. Figure includes: (A) all mammal species in study, (B) amplification of medium-sized mammals in study, (C) amplification of small mammals in study. Bongo, Pygmy hippopotamus and Bengal tiger were excluded due to sample size or lack of standard photograph angles.

Table 2. Group specific predictive equations (GPE; Eq. 2) to approximate body mass: R^2 values are the result of linear regression fit of measured mass (ME) to predicted photogrammetric body mass.

Groups	Photos	Range MBM (kg)	% ME overestimate (mean ± SD)	Equation	% PBM error (mean ± SD)	n	R^2
Primates	10	47–112	32.01 ± 4.9	PBM = ME − [ME × (0.242 ± 0.029)]	0.13 ± 3.8	7	0.99
Hindgut fermenters	10, 12	223–4060	19.9 ± 3.9	PBM = ME − [ME × (0.166 ± 0.027)]	0.08 ± 3.2	38	0.99
Foregut fermenters	10	56–284	11.8 ± 3.4	PBM = ME − [ME × (0.105 ± 0.027)]	0.08 ± 3.1	9	0.99
Ruminants	10	70–264	24.0 ± 3.5	PBM = ME − [ME × (0.189 ± 0.060)]	0.58 ± 7.8	22	0.98
Carnivores	10	35–204	11.8 ± 3.6	PBM = ME − [ME × (0.241 ± 0.053)]	−0.90 ± 7.1	16	0.98

Note: PBM: predicted body mass (kg); ME: mass estimate from photogrammetric volume (kg); n: sample size; MBM: measured body mass; mean and standard deviation (SD) are indicated.

and ruminants. Consistency in percentage overestimation in groups, advocates a group specific predictive equation, to correct for such constant overestimation (Table 2). Group specific predictive equations (GPE) were calculated as:

$$\text{GPE} = \sum \frac{1 - (\frac{\text{MBM}}{\text{ME}})}{n} \quad (2)$$

where MBM is measured body mass. Group specific predictive equations were applied to ME to calculate group specific predicted body mass (GPBM):

$$\text{PBM} = \text{ME} - [\text{ME} \times (\text{GPE} \pm \text{SD})]. \quad (3)$$

Further distinction was made by dividing digestive groups into species to address variation in GPBM percentage overestimation in carnivores and ruminants (Table 2). Species-specific predictive equations (SPE), Eq. 4, were calculated for 13 species, excluding bongo, pygmy hippopotamus and Bengal tiger ($n = 1$) which were excluded for lack of standard photograph angles (Table 3).

$$\text{SPE} = \sum \frac{1 - (\frac{\text{MBM}}{\text{ME}})}{n}. \quad (4)$$

Predictive values were applied to each species, Eq. 5, to obtain species-specific predicted body mass (SPBM):

$$\text{SPBM} = \text{ME} - [\text{ME} \times (\text{SPE} \pm \text{SD})]. \quad (5)$$

Missing silhouettes

A combination of photographs were systematically removed from each project (e.g., front-view, back-view and front-view, one whole side view) to imitate field scenarios where natural obstacles prevent photographs from certain

Table 3. Species specific predictive equations (SPE; Eq. 4) to approximate body mass: R^2 values are the result of linear regression fit of measured mass (ME) to predicted photogrammetric body mass.

Species	Photos	Range MBM (kg)	% ME overestimate (mean ± SD)	Equation	% PBM error (mean ± SD)	n	R^2
Arabian oryx	10	45–60	41.1 ± 5.4	PBM = ME − [ME × (0.291 ± 0.027)]	0.06 ± 3.8	3	0.99
Bengal tiger	10	109–114	48.6 ± 0.1	PBM = ME − [ME × (0.304 ± 0.011)]	0.01 ± 1.5	2	...
Cheetah	10	35–49	40.3 ± 2.5	PBM = ME − [ME × (0.287 ± 0.013)]	0.03 ± 1.8	5	0.97
Chimpanzee	10	47–87	29.7 ± 5.3	PBM = ME − [ME × (0.229 ± 0.032)]	0.03 ± 4.1	2	...
Hyena	10	53–78	24.0 ± 3.6	PBM = ME − [ME × (0.193 ± 0.024)]	0.07 ± 2.9	4	0.99
Lion	10	114–204	25.3 ± 4.9	PBM = ME − [ME × (0.201 ± 0.031)]	0.09 ± 3.9	5	0.99
Nyala	10	36–71	17.6 ± 4.7	PBM = ME − [ME × (0.148 ± 0.027)]	0.20 ± 4.0	9	0.96
Red river hog	10	56–75	11.4 ± 3.4	PBM = ME − [ME × (0.101 ± 0.026)]	0.1 0 ± 3.0	8	0.91
Sable antelope	10	170–221	15.4 ± 4.8	PBM = M − [ME × (0.133 ± 0.036)]	0.05 ± 4.2	2	...
Springbok	10	25–38	25.7 ± 4.3	PBM = ME − [ME × (0.204 ± 0.028)]	0.05 ± 4.2	7	0.97
Western lowland gorilla	10	60–112	32.9 ± 5.1	PBM = ME − [ME × (0.265 ± 0.051)]	0.88 ± 3.9	5	0.95
Zebra	10	223–298	18.7 ± 1.7	PBM = ME − [ME × (0.158 ± 0.012)]	−0.04 ± 1.0	3	0.99
Elephant	12	1650–4060	22.7 ± 5.1	PBM = ME − [ME × (0.184 ± 0.036)]	0.11 ± 4.1	9	0.98
White rhino	12	548–1970	19.2 ± 3.2	PBM = ME − [ME × (0.161 ± 0.024)]	0.00 ± 2.7	26	0.99

Note: PBM: predicted body mass (kg); ME: mass estimate from photogrammetric volume (kg); n: sample size; MBM: measured body mass; mean and standard deviation (SD) are indicated.

Table 4. Missing silhouettes scenarios: Representation of silhouettes removed from each project to replicate field scenarios that might occur as a result of natural obstacles that prohibit certain photo angles to be taken.

Photo scenarios	Camera angles excluded from model
12	None
11	12
10	11, 12
9	10, 11, 12
8	9, 10, 11, 12
7h	6, 9, 10, 11, 12
7f	1, 9, 10, 11, 12
7b	5, 9, 10, 11, 12
7s	7, 9, 10, 11, 12
6a	2, 6, 9, 10, 11, 12
6b	3, 4, 9, 10, 11, 12
6c	3, 7, 9, 10, 11, 12
6d	1, 4, 9, 10, 11, 12
6e	6, 8, 9, 10, 11, 12
5a	6, 7, 8, 9, 10, 11, 12
5b	1, 2, 8, 9, 10, 11, 12
5c	1, 2, 3, 9, 10, 11, 12
4a	1, 2, 3, 4, 9, 10, 11, 12
4b	1, 2, 7, 8, 9, 10, 11, 12
3a	1, 2, 3, 4, 5, 9, 10, 11, 12
3b	3, 4, 5, 6, 7, 9, 10, 11, 12

Note: Photo scenario refers to the number of photos used in the model and letters refer to which combinations of angles are excluded from the PG model (Figs. 1 and 7).

angles being taken (Fig. 1; Table 4). This enabled the simulation of different field scenarios ($n = 18$, for animals smaller than 300 kg and $n = 20$, for animals larger than 300 kg) per individual. Predictive equations for each scenario (Appendix A: Tables A1 and A2) could be calculated for each species as illustrated in Eq. 2.

Statistical analysis

The program R, version 2.13.1 (R Core Team 2011) was used for statistical analysis. Normality was tested using a Shapiro-Wilks test, and if absent, data were log transformed. An implementation of the Grammar of Graphics (ggplot2; Wickham and Chang 2013) was used for graphic illustration. Analysis of variance (ANOVA) was used to assess percentage overestimation (after log transformation) between different digestive groups, followed by a post hoc Tukey HSD test. Photogrammetrically predicted species mass estimates (PBM) versus physically weighed mass (MBM) was plotted to calculate the coefficient of determination. To assess PBM accuracy within species if data were normally distributed, *t* tests were used; conversely a Wilcoxon test was performed. Predicted body mass was compared to MBM (regardless of species) with a Kruskal-Wallis test. An *F* test for variance was applied between percentage GPBM and SPBM if data were normally distributed; conversely a Wilcoxon test was performed. Significance was set at $p < 0.05$, and means are reported with standard deviation (SD).

Results

Measured body mass ranged from 25 to 4060 kg (Tables 2 and 3). Results indicate a robust mass estimation method. Despite overestimation, mass was consistently predicted within narrow confidence limits allowing simple and confident correction. Predicted versus actual measured mass estimations showed a strong linear relationship ($R^2 = 0.91$–0.99, depending on the species).

Different digestive groups PBM vs. species PBM

Percentage overestimation within digestive groups ranged from 11.8% to 32.0% and variation

Table 5. Percentage overestimation: Percentage over estimation of mass estimate (ME) compared between digestive groups, results obtained from a one-way ANOVA.

Interaction	diff	lwr	upr	*p*
Foregut-carnivores	−1.01	−1.33	−0.68	*** < 0.0001
Hindgut-carnivores	−0.46	−0.70	−0.23	*** < 0.0001
Primates-carnivores	0.02	−0.34	0.37	0.9999
Ruminants-carnivores	−0.34	−0.60	−0.08	**0.0041
Hindgut-foregut	0.54	0.25	0.84	*** < 0.0001
Primates-foregut	1.02	0.63	1.42	*** < 0.0001
Ruminants-foregut	0.67	0.36	0.98	*** < 0.0001
Primates-hindgut	0.48	0.15	0.80	**0.0008
Ruminants-hindgut	0.12	−0.09	0.33	0.4726
Ruminants-primates	−0.35	−0.69	−0.01	0.0383

Note: Mean difference (diff), lower (lwr) and upper (upr) limits and *p* values (*p*) are presented.

Table 6. Group specific test statistics: Group specific measured body mass (MBM) vs. predicted body mass (PBM).

Groups	*n*	Test	*w*	*t*	df	*p*
Primates	7	*t* test	NA	0.02	11.99	0.98
Hindgut fermenters	38	Wilcoxon	715	NA	NA	0.95
Foregut fermenters	9	Wilcoxon	37	NA	NA	0.79
Ruminants	22	Wilcoxon	239	NA	NA	0.95
Carnivores	16	Wilcoxon	132	NA	NA	0.90

Note: Test statistic; (*t*) for *t* test, (*w*) for non-parametric Wilcoxon test, degrees of freedom (df), *p* values (*p*), sample size (*n*) are presented.

(SD) around overestimation ranged from ±3.4% to ±4.9% (Table 2). Significant differences were present between digestive groups' percentage overestimation (calculated from ME, before correction; ANOVA; Table 5). No significant difference was present between PBM and MBM in any digestive groups ($p = 0.79$–0.98, depending on group; Table 6). However, variance in percentage PBM error is double for ruminants and carnivores (mean 0.58 ± 7.8% and −0.89 ± 7.18%) to that of primates and fore-and-hindgut fermenters (0.133 ± 3.772%, 0.079 ± 3.213% and

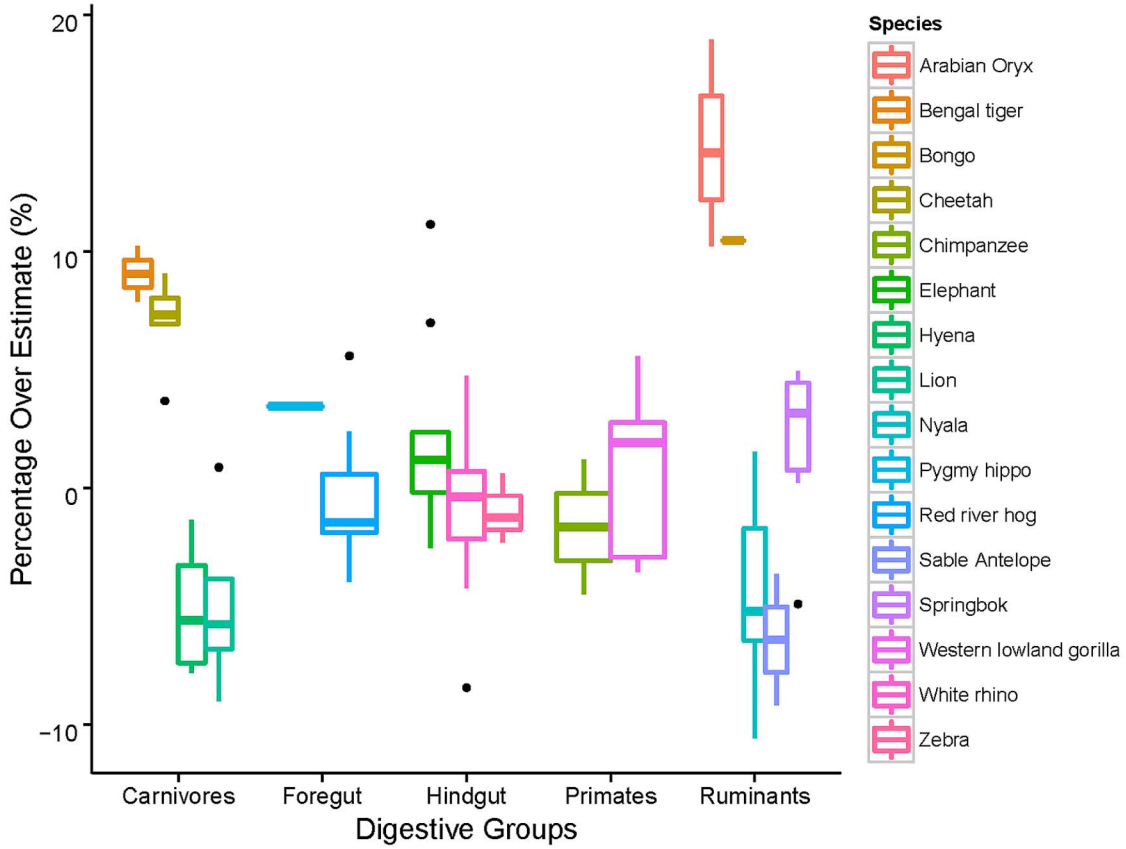

Fig. 3. Percentage predicted body mass (PBM) error from digestive group correction equation: Individual species within primates, hind-and-foregut fermenters are consistently overestimated as a group with the de Bruyn et al. (2009) volumetric mass estimation method. Individual species within the digestive groups; carnivores and ruminants are however not consistently overestimated. Percentage overestimate is demonstrated by box-and-whisker plots (median and inter-quartile range are displayed).

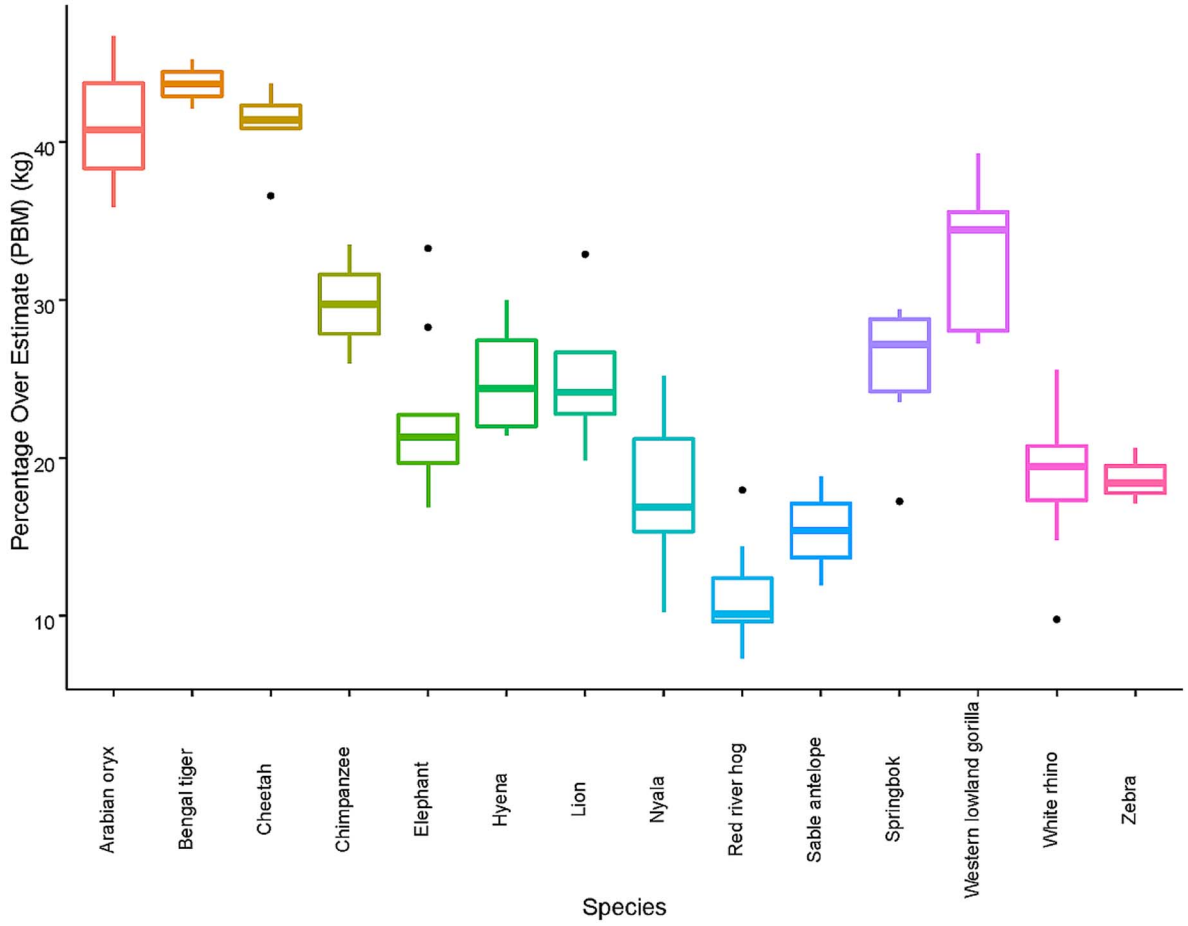

Fig. 4. Percentage over estimation from Mass estimate (ME): individuals within a species are consistently overestimated with the de Bruyn et al. (2009) volumetric mass estimation method. Percentage overestimate is demonstrated by box-and-whisker plots (median and inter quartile range are displayed).

Table 7. Species specific test statistics: species specific measured body mass (MBM) vs. predicted body mass (PBM).

Species	*n*	Test	*w*	*t*	df	*p*
Arabian oryx	3	*t* test	NA	0.03	3.84	0.98
Bengal tiger	2	*t* test	NA	0.01	1.63	1.00
Cheetah	5	*t* test	NA	−0.06	8.00	0.95
Chimpanzee	2	*t* test	NA	−0.02	1.98	0.99
Hyena	4	*t* test	NA	−0.09	5.88	0.94
Lion	5	Wilcoxon	13	NA	NA	1.00
Nyala	9	*t* test	NA	−0.04	15.80	0.97
Red river hog	8	*t* test	NA	0.00	13.89	1.00
Sable antelope	2	*t* test	NA	0.02	1.88	0.99
Springbok	7	*t* test	NA	0.04	11.60	0.97
Western lowland gorilla	5	Wilcoxon	16	NA	NA	0.53
Zebra	3	*t* test	NA	0.00	3.99	1.00
Elephant	9	*t* test	NA	0.01	15.98	0.99
White rhino	26	*t* test	NA	−0.03	49.96	0.98

Note: Test statistic (*t*) for *t* test, (*w*) for non-parametric Wilcoxon test, degrees of freedom (df), *p* values (*p*), sample size (n) are presented.

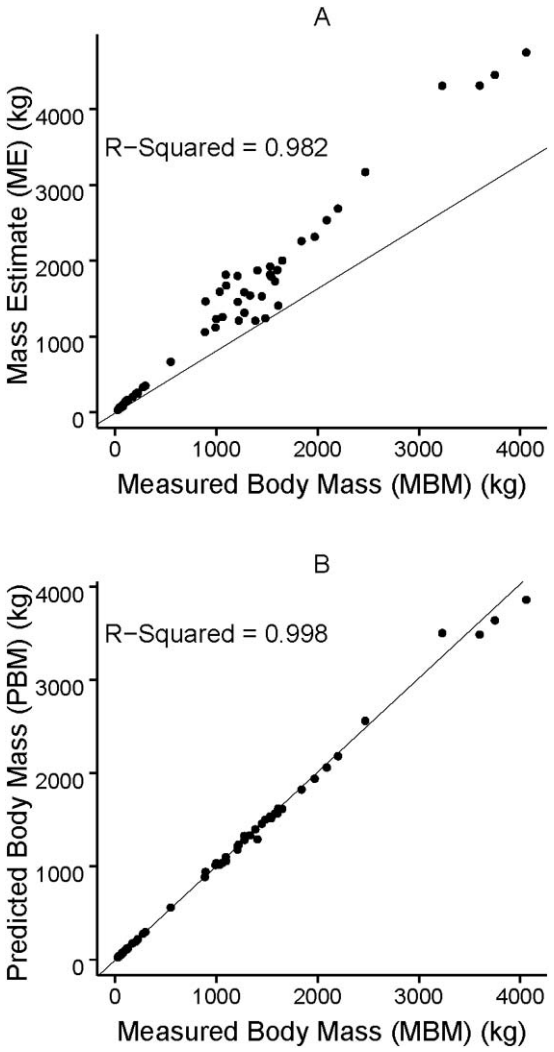

Fig. 5. (A) Mass estimate (ME) plotted against physically measured mass (PBM): of 13 species ranging from 25 to 4060 kg ($R^2 = 0.982$) and (B) Predicted body mass (PBM) estimated by photogrammetry plotted against physically measured body mass (MBM) of 13 species ranging from 25 to 4060 kg ($R^2 = 0.998$).

0.078 ± 3.082%; Table 2, Fig. 3). No significant difference was present between PBM error for digestive group (Eq. 3) and species (Eq. 5) for primates ($F = 0.9583$, df = 6, $p = 0.96$), foregut fermenters ($F = 0.9067$, df = 8, $p = 0.89$) and hindgut fermenters ($w = 734$, $p = 0.90$). However a significant difference was present for ruminants ($F = 0.1947$, df = 21, $p = 0.0004$) and carnivores ($F = 0.1526$, df = 15, $p = 0007$).

The species ME equation consistently overestimated the mass of individuals within a species, with little variation in the percentage overestimation between individuals (Fig. 4). Species percentage overestimation ranged from 11.4% to 48.6% and variation (SD) around overestimation ranged from ±0.1% to ±5.4%. No significant difference was present between PBM and MBM in any species (ranging from $p = 0.53$ to $p = 0.99$, depending on species) (Table 7). The goodness of fit for species PBM was assessed by the coefficient of determination from a linear model; photogrammetric predicted mass estimation (PBM) versus physically measured body mass (MBM; Fig. 5) with an $R^2 = 0.99$, df = 87, $t = -0.497$. Finally percentage PBM errors were assessed by plotting the percentage under/overestimation for each species (Fig. 6, Tables 2 and 3).

Missing silhouettes

The optimal number of silhouettes (maximum of one per photograph) required to provide an accurate 3D model (once cross-referenced between photographs) of animals weighing less than 300 kg, was 10 (Fig. 2). Larger animals such as white rhinoceros and African elephant required 12 cross-referenced silhouettes to provide an accurate mass estimation (Fig. 2). PBM accuracy improved with increased number of photographs (Fig. 7). Species-specific corrective equations for specific missing silhouettes scenarios and mass overestimation (e.g., 3a, 5b, 7h, etc.; Appendix A: Tables A1 and A2) decreased with an increase in number of photographs cross-referenced per animal (Appendix B).

Discussion

Application of the de Bruyn et al. (2009) method to 16 terrestrial species showed similar findings to the original southern elephant seal application. The volume of individuals within each species was consistently overestimated by the method; however the extent of the overestimation differed among digestive groups and from that of the southern elephant seals. This variance is consistent with the described range of species specific photogrammetry methods linked to the varied species morphologies (e.g., limb length and fur thickness, etc.). Importantly,

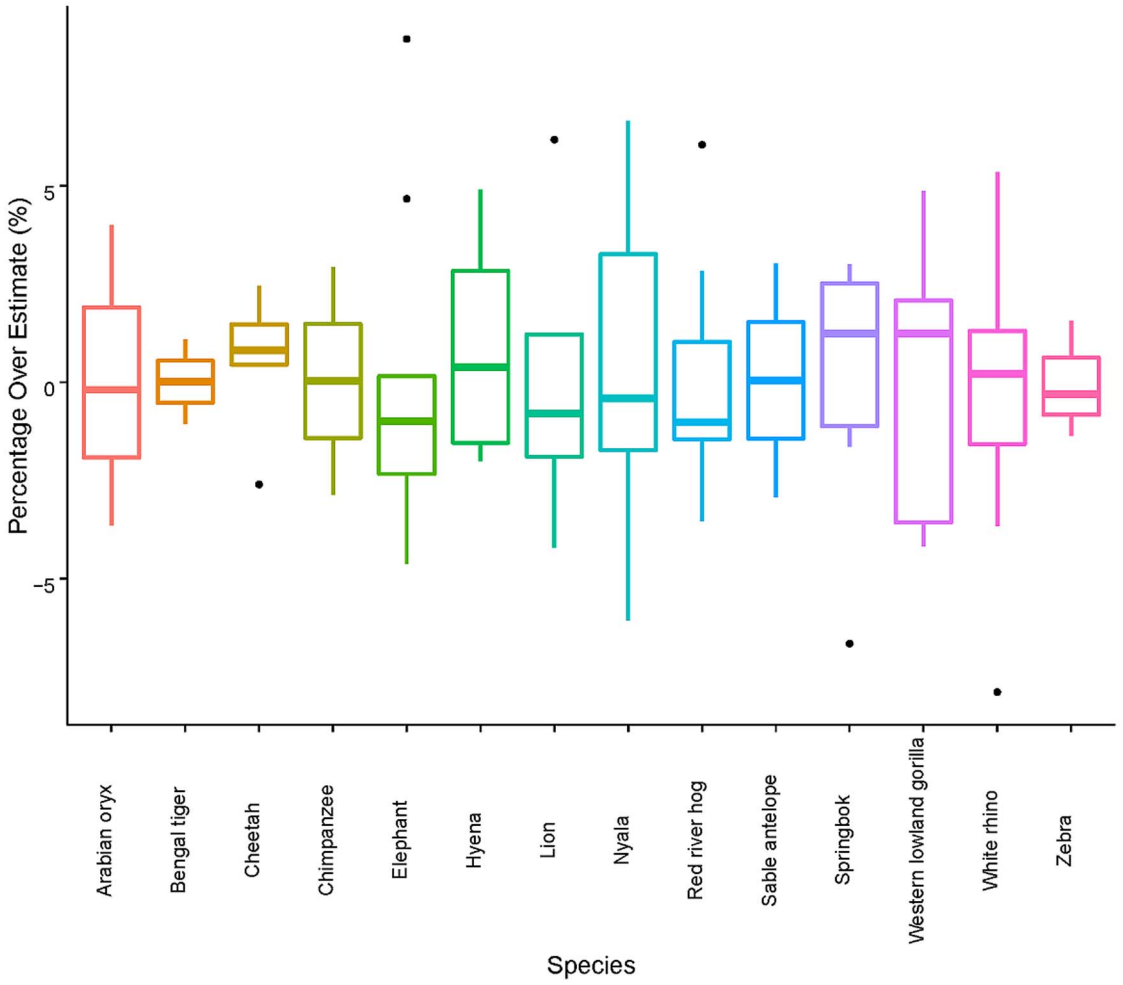

Fig. 6. Percentage predicted body mass (PBM) error: demonstrated by Box-whisker plots (median, inter quartile range and outliers are displayed).

although there was variation in volumetric overestimation among different digestive groups, there was little variation between individuals within each digestive group, with the exception of carnivores and ruminants. Variation within carnivores and ruminants necessitated the application of a species-specific predictive equation rather than a group-specific equation. Consistency within species supports the application of species-specific predictive equations that provide confident correction to estimates (Table 3). Thus, the same field method can be applied to any species and accurate volume and mass estimates can be obtained provided that initial calibration is done with known mass individuals for a species that has not been sampled previously.

In essence then, we find support for the proposed multispecies application of the de Bruyn et al. (2009) method, but also show that species-specific calibration (i.e., photogrammetry 3D model derivatives compared to actually weighed individuals) remains important for accurate application to some species. Encouragingly, we do show congruence in estimates from species of similar functional/digestive groups. We explored the advantages and limitations of this photogrammetric method in a controlled environment. The systematic removal of silhouettes from models enabled us to simulate potential field scenarios ($n = 20$) where certain camera angles may not be available for an individual in the field. Missing silhouettes result

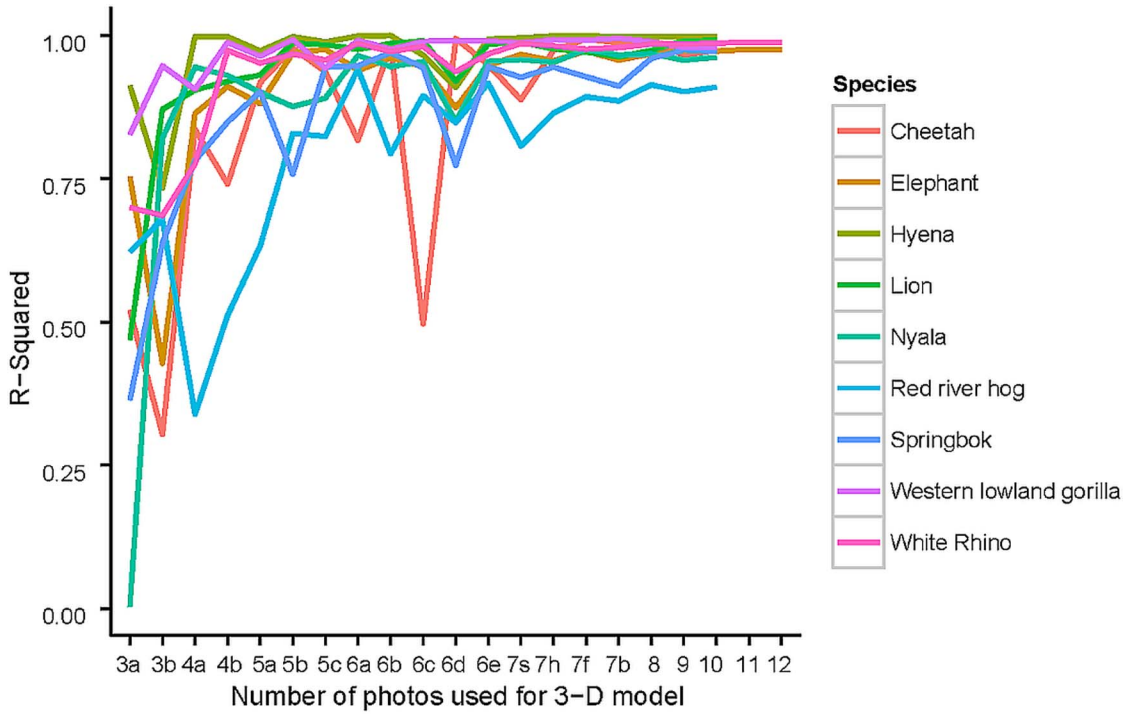

Fig. 7. Species-specific coefficients of determination: values are the result of linear regression fit of measured mass to predicted photogrammetric body mass. Number of cross-referenced silhouettes is represented by the numbers on *x*-axis, alphabetic letters following number of cross-referenced silhouettes represents specific scenarios (specified Table 3) with amount of silhouettes specified. Species with only two samples were excluded.

in an overestimation of the extent of the object, due to an insufficient number of angles to allow the software to accurately define the 3D model of the animal. High angled photographs are especially useful; these enable the software to define limbs realistically. The combination of the front and back silhouettes (Fig. 7: 6c, Table 4) are essential in a 3D model to accurately assign PBM. Realistic and accurate PBM could be achieved from six silhouettes; but accuracy increased with the number of silhouettes cross-referenced.

The accuracy of the method did not vary with sample size, species with a small number or large number of samples showed similar R^2 values for PBM versus MBM (Arabian oryx $n = 3$, $R^2 = 0.99$; and white rhino $n = 26$, $R^2 = 0.99$). The only species with an R^2 lower than 0.95 (PBM vs. MBM) was the Red river hog. However the percentage PBM error for this species is small (mean = 0.102; SD $\pm 3.019\%$). Furthermore, even mammals with complex body morphology (e.g., primates) could be accurately assessed. The method is especially useful for large mammals (e.g., rhinoceros and elephants), which are always difficult to weigh, even in captive or manipulated scenarios. The method accuracy is however subject to the visibility and resultant cross-referencing of substrate markers for orientation of photographs in 3D space. Substrate markers can be obscured in a field scenario either by the subject itself, (e.g., elephants, due to their large size) or by natural obstacles (e.g., trees, grass and rocks), and the photographer needs to bear this in mind while taking photographs in the field.

Evidence that (1) multiple cameras can be used with simultaneous shutter-release to effectively 'freeze' a mobile animal in time (Waite et al. 2007), combined with (2) the ability to use substrate and surrounding environment to accurately define a 3D space (de Bruyn et al. 2009) and (3) support for multispecies assessment with a single technique, provide promise for the development of a truly field orientated setup

capable of remotely assessing morphometrics, body volume, size and mass of multiple mammalian species without immobilization or manipulation. Already, given an immobile subject (e.g., during veterinary procedures in remote field locations) the technical merits of this photogrammetry method are numerous: including (1) accuracy of mass estimation, (2) single operator is required, which facilitates the ease of field work (3) light-weight portable equipment that facilitates field use, (4) no need for exactly delineated camera positions and/or distances, as long as the subject is photographed from various angles.

Conclusion

This method provides significant progress towards accurately assessing body mass of a wide variety of terrestrial mammals with the use of photographs. The ability to estimate the body mass of any animal by using a single photogrammetric method would be useful to biologists conducting research in remote areas or with limited research budgets. The knowledge field is poised for future developments in ascertaining the technical feasibility of a multiple-camera field setup that incorporates these and earlier findings for truly 'hands-off' collection of morphometric, body size and mass information for wild mammals. Furthermore, incorporating 3D camera photogrammetry and conventional camera trapping could allow photographic mark-recapture of individuals with the addition of size/mass covariates to facilitate population demographic modeling. This method provides fundamental progress towards wide application and contribution of vital life history parameter data for research efforts focused on monitoring populations and ultimately ecological interactions.

Acknowledgments

We thank the South African National Parks and the National Zoological Gardens of South Africa for fieldwork access. We thank the Department of Science and Technology via the National Research Foundation (NRF), and the University of Pretoria for funding. Thanks to Chris Oosthuizen for data gathering field assistance. We dedicate this paper to our late friend and colleague Greg Fleming, whose infectious enthusiasm for wildlife in general and eagerness for photogrammetric progress is and will continue to be deeply missed.

Literature Cited

Alexander, R. M., and G. Goldspink. 1977. Mechanics and energetics of animal locomotion. Chapman and Hall, London, UK.

Baker, W. H. 1960. Elements of photogrammetry. Ronald Press, New York, New York, USA.

Bell, C. M., M. A. Hindell, and H. R. Burton. 1997. Estimation of body mass in the southern elephant seal, *Mirounga leonina*, by photogrammetry and morphometrics. Marine Mammal Science 13:669–682.

Berger, J. 2012. Estimation of body-size traits by photogrammetry in large mammals to inform conservation. Conservation Biology 26:769–777.

Bergeron, P. 2007. Parallel lasers for remote measurements of morphological traits. Journal of Wildlife Management 71:289–292.

Cagnacci, F., L. Boitani, R. A. Powell, and M. S. Boyce. 2010. Challenges and opportunities of using GPS-based location data in animal ecology. Philosophical Transactions of the Royal Society B 365:1550.

Clutton-Brock, T. H., S. D. Albon, and F. E. Guinness. 1989. Fitness costs of gestation and lactation in wild mammals. Nature 337:260–262.

Costa, D. P., G. A. Breed, and P. W. Robinson. 2012. New insights into pelagic migrations: implications for ecology and conservation. Annual Review of Ecology and Evolution Systematics 43:73–96.

De Bruyn, P. J. N., M. N. Bester, A. R. Carlini, and W. C. Oosthuizen. 2009. How to weigh an elephant seal with one finger: a simple three-dimensional photogrammetric application. Aquatic Biology 5:31–39.

Deng, G., and W. Faig. 2001. An evaluation of an off-the-shelf digital close-range photogrammetric software package. International Society for Photogrammetry and Remote Sensing 67:227–233.

Durnin, J. V. G. A., and J. Womersley. 1974. Body fat assessed from total body density and its estimation from skinfold thickness: measurements on 481 men and women aged from 16 to 72 years. British Journal of Nutrition 32:77–97.

Festa-Bianchet, M., J.-M. Gaillard, and J. T. Jorgenson. 1998. Mass and density dependent reproductive success and reproductive costs in a capital breeder. American Naturalist 152:367–379.

Gaillard, J.-M., J.-M. Boutin, D. Delorme, G. Van Laere, P. Duncan, and J.-D. Lebreton. 1997. Early survival in roe deer: causes and consequences of cohort variation in two contrasted populations. Oecologia 112:502–513.

Gaillard, J.-M., M. Festa-Bianchet, N. G. Yoccoz, A. Loison, and C. Toïgo. 2000. Temporal variation in fitness components and population dynamics of

large herbivores. Annual Review of Ecology and Systematics 31:367–393.

Haley, M. P., C. J. Deutsch, and B. J. Le Boeuf. 1991. A method for estimating mass of large pinnipeds. Marine Mammal Science 7:157–164.

Ireland, D., R. A. Garrott, J. Rotella, and J. Banfield. 2006. Development and application of a mass-estimation method for Weddell seals. Marine Mammal Science 22:361–378.

Keith, M., M. N. Bester, P. A. Bartlett, and D. Baker. 2001. Killer whales (*Orcinus orca*) at Marion Island, Southern Ocean. African Zoology 36:163–175.

Lambertsen, R. H., K. J. Rasmussen, W. C. Lancaster, and R. J. Hintz. 2005. Functional morphology of the mouth of the bowhead whale and its implications for conservation. Journal of Mammalogy 86:342–352.

Lindstedt, S. L., and M. S. Boyce. 1985. Seasonality, fasting endurance, and body size in mammals. American Naturalist 125:873–878.

McCallum, J. 2013. Changing use of camera traps in mammalian field research: habitats, taxa and study types. Mammal Review 43:196–206.

McMahon, C. R., H. R. Burton, and M. N. Bester. 2000. Weaning mass and the future survival of southern elephant seals, *Mirounga leonina*, at Macquarie Island. Antarctic Science 12:149–154.

Postma, M., M. N. Bester, and P. J. N. de Bruyn. 2013*a*. Spatial variation in female southern elephant seal mass change assessed by an accurate non-invasive photogrammetry method. Antarctic Science 25:731–740.

Postma, M., M. N. Bester, and P. J. N. de Bruyn. 2013*b*. Age-related reproductive variation in a wild marine mammal population. Polar Biology 36:719–729.

Purves, D., J. Charlemann, M. Harfoot, T. Newbold, D. P. Tittensor, J. Hotton, and S. Emmoot. 2013. Time to model all life on earth. Nature 493:295–297.

R Core Team. 2013. R: a language and environment for statistical computing. R Foundation for Statistical Computing, Vienna, Austria.

Remondino, F., and C. Fraser. 2006. Digital camera calibration methods: considerations and comparisons. International Society for Photogrammetry and Remote Sensing 36:266–272.

Rothman, J. M., C. A. Chapman, D. Twinomugisha, M. D. Wasserman, J. E. Lambert, and T. L. Goldberg. 2008. Measuring physical traits of primates: the use of parallel lasers. American Journal of Primatology 70:1191–1195.

Shrader, A. M., S. M. Ferreira, and R. J. van Aarde. 2006. Digital photogrammetry and laser rangefinder techniques to measure African elephants. South African Journal of Wildlife Research 36:1–7.

Trimble, M. J., R. J. van Aarde, S. M. Ferreira, C. F. Nørgaard, J. Fourie, P. C. Lee, and C. J. Moss. 2011. Age determination by back length for African savanna elephants: extending age assessment techniques for aerial-based surveys. PLoS ONE 10:e26614.

Waite, J. N., W. J. Schrader, J. E. Mellish, and M. Horning. 2007. Three-dimensional photogrammetry as a tool for estimating morphometrics and body mass of Steller sea lions (*Eumetopias jubatus*). Canadian Journal of Fisheries and Aquatic Science 64:296–303.

Wang, Z., P. Deurenberg, W. Wang, A. Pietrobelli, R. N. Baumgartner, and S. B. Heymsfield. 1999. Hydration of fat-free body mass: review and critique of a classic body-composition. American Journal of Clinical Nutrition 69:833–841.

Wickham, H., and W. Chang. 2013. ggplot2: an implementation of the Grammar of Graphics. R package version 0.9.3.1. http://ggplot2.org, https://github.com/hadley/ggplot

Williams, R. J., and N. D. Martinez. 2000. Simple rules yield complex food webs. Nature 404:180–183.

Zedrosser, A., F. Pelletier, R. Bischof, M. Festa-Bianchet, and J. E. Swenson. 2013. Determinants of lifetime reproduction in female brown bears: early body mass, longevity, and hunting regulations. Ecology 94:231–240.

Supplemental Material

Ecological Archives

Appendices A and B are available online: http://dx.doi.org/10.1890/ES15-00368.1.sm